Synthetic Metals 196 (2014) 173–177

Contents lists available at ScienceDirect

Synthetic Metals

journal homepage: www.elsevier.com/locate/synmet

Polypyrrole nanotube film for flexible thermoelectric application

Jiansheng Wu[a], Yimeng Sun[b], Wen-Bo Pei[c], Ling Huang[c], Wei Xu[b,**], Qichun Zhang[a,*]

[a] School of Materials Science and Engineering, Nanyang Technological University, 50 Nanyang Ave, Singapore 639672, Singapore
[b] Beijing National Laboratory for Molecular Sciences, Laboratory of Organic Solids, Institute of chemistry, Chinese Academy of Sciences, Beijing 100190, PR China
[c] Jiangsu-Singapore Joint Research Center for Organic/Bio-Electronics & Information Displays and Institute of Advanced Materials (IAM), Nanjing Tech University, Nanjing 211816, PR China

ARTICLE INFO

Article history:
Received 2 July 2014
Received in revised form 29 July 2014
Accepted 3 August 2014
Available online 23 August 2014

Keywords:
Electrical conductivity
Self-assembly
Conducting polymers
Film
Thermoelectric effects

ABSTRACT

Flexible and lightweight organic thermoelectric (TE) devices have potential applications in self-powered health monitoring for humans and wearable self-powered gas/chemical detection. Two flexible and free-standing polypyrrole (PPy) nanotube films (PPy-1 and PPy-2) have been fabricated and the structures, morphologies and thermoelectric properties of the as-prepared PPy films have been carefully investigated. Our results show that the smaller size and longer length of PPy nanotubes are helpful to enhance the electrical conductivity and Seebeck coefficient while size and length have less effect on thermal conductivity.

1. Introduction

The energy crisis, green-house effect, and enormous amounts of unused waste heat (generated by industry, home heating, and automotive exhaust) have created a strong demand for high-efficient heat-to-electric generators. Thermoelectric (TE) devices are such a device, which can directly convert heat into electrical energy without complicated structures and moving parts, and vice versa [1–5]. Traditional TE materials are heavily dependent on low bandgap inorganic semiconductors such as bismuth chalcogenides, lead telluride and tin selenide and their ZT value (an important factor to evaluate TE materials) can be as high as 2.2 [6–8]. Recently, organic TE materials have received a lot of research interests because these materials have their own advantages such as low density, low thermal conductivity, low cost, and easy to synthesize or process [9–13]. Although the thermal stability of organic TE materials (most are TE polymers) cannot support them to be used in medium and high temperature, *on-demand* cooling and low-end waste heat management under low temperature could be their main focus [14]. In addition, theoretical study has already shown that TE performance of quasi-one-dimensional (1D) organic crystals at room temperature could reach a very high value if they could linearly stack into one chain and then furthermore pack into a 3D crystal [15–17]. Recently, the development of flexible and lightweight organic TE devices has attracted great attention due to their potential applications in self-powered health monitoring for humans and wearable self-powered gas/chemical detection without wiring [18–21]. However, most of the reported flexible TE devices are based on carbon nanotubes (CNTs) and graphene, whose prices have posed a limitation for their practical applications.

As one member of conducting polymer family, polypyrrole (PPy) has attracted much interest as a promising TE candidate owing to its facile synthesis, no toxicity, good electrical conductivity and low thermal conductivity [22–26]. However, using PPy nanotubes as TE materials is rare. In addition, how the size and length of PPy nanotubes to affect the TE performance (e.g. electrical conductivity and Seebeck) is still unclear. In this paper, for the first time, we fabricated free-standing PPy nanotube-based films for TE applications. The structures, morphologies and thermoelectric properties of the as-prepared PPy films have been carefully investigated. Our results show that the flexible free-standing PPy nanotube films have good mechanical properties and considerable TE performance.

2. Experimental

2.1. Preparation of PPy nanotube

The PPy nanotubes were prepared through two similar self-degraded template methods [25,26]. In method one, 10 mL HCl

* Corresponding author. Tel.: +65 67904705; fax: +65 67909081.
** Corresponding author.
E-mail addresses: wxu@iccas.ac.cn (W. Xu), qczhang@ntu.edu.sg (Q. Zhang).

http://dx.doi.org/10.1016/j.synthmet.2014.08.001
0379-6779/

solution (2 M) was added into 300 mL methyl orange (MO) DI water solution (5 mM). Then, 0.56 mL pyrrole (Py) monomer was put into the mixture solution. After stirring for 10 min, the aqueous solution (20 mL) containing 2.5 g Iron (III) chloride hexahydrate ($FeCl_3{\cdot}6H_2O$) was dropped into the above solution. Then, the resulted mixture was kept stirring for 4 h at room temperature. In method two, about 2.6 g of $FeCl_3{\cdot}6H_2O$ was added to 320 mL MO DI water solution (5 mM). After stirring for 20 min, 0.5 mL Py monomer was dropped into the mixture solution, followed by stirring for 4 h at room temperature. The precipitated PPy nanotubes from two methods were washed several times with DI water and ethanol until the filtrate became colorless and neutral.

2.2. Preparation of free-standing PPy nanotube film

The PPy nanotubes were dispersed into 1 M HCl (volume) and stirred for 12 h at room temperature before use. PPy nanotubes were centrifuged and rinsed by deionized water and ethanol. The resulted nanotubes were dispersed in ethanol again and the suspension was poured into a glass petri dish. The glass petri dish was dried in an oven at 60 °C for 12 h. The PPy-1 and PPy-2 nanotube films were obtained through the self-assembly of PPy nanotubes (by method one and two) during the evaporation of ethanol. Two free-standing PPy films (PPy-1 and PPy-2) have black color with smooth surfaces, which are flexible and mechanically robust (Fig. 1).

2.3. Characterization

Fourier transform infrared spectra (FT-IR) were recorded on a PerkinElmer Spectrum BX FT-IR spectrometer. The thermogravimetric analysis (TGA) was recorded by TA Instruments TGA 2950 under a nitrogen flow (40 mL/min) with a heating rate of 10 °C/min. The X-ray diffraction (XRD) patterns were measured by a Bruker D2 Phaser X-ray diffractometer with Cu Kα radiation (λ = 1.5406 Å) from 5° to 60° at a step of 0.1°/s. FESEM was performed on a JEOL/JSM-6340F with an acceleration voltage of 5 kV. TEM measurements were carried out using a JEOL JEM-1400 transmission electron microscope operating at an accelerating voltage of 100 kV.

2.4. Thermoelectric properties measurement

The Seebeck coefficient and electrical conductivity were measured by SB-100 Seebeck Measurement System (MMR Tech.) and KEITHLEY 2002 Multimeter (Keithley Instrument Inc.), respectively. The free-standing PPy films were cut into rectangle shape (2 × 5 mm) for electrical conductivity and Seebeck coefficient measurement. The thermal conductivity was measured by TCi Thermal Conductivity Analyzer (C-THERM Tech.). The samples were compressed into a disk-like pellet with diameters of 17 mm, and thickness of 1–2 mm for thermal conductivity measurement.

3. Results and discussion

The FT-IR spectra of the PPy films (Fig. S1 Supporting Information) showed characteristic peaks at 1515, 1432, 1277, 1111, 1080 and 1004 cm^{-1}, which are similar to those reported for PPy [27]. The bonds around 1515 and 1432 cm^{-1} are assigned to the C—C and C—N stretching vibrations in the pyrrole ring, respectively. The broad band at 1277 cm^{-1} is attributed to C—H or C—N in-plane deformation modes. The bonds around 1111, 1080 and 1000 cm^{-1} are attributed to the C—H and N—H in-plane deformation. The X-ray diffraction patterns of PPy-1 and PPy-2 films were shown in Figure S2. In general, the X-ray diffraction patterns of PPy particles show a broad scattering peak in the range of 2θ = 15–30° [28]. In our research, two main peaks were observed at 18 and 26.5°, which indicated the good crystallization characteristics of our as-prepared PPy tubes. The peak centered at 2θ = 26.5° of PPy-2 films, corresponding to the inter-planar spacing of the pyrrole chains, appears sharper than that of PPy-1 membrane, indicating a more ordered pyrrole chain structure [27,28].

The TEM images of the different PPy nanotubes (Fig. 2) showed that the diameters of PPy-1 and PPy-2 nanotubes are about 300 and 80 nm, respectively. The length of PPy-1 tubes is shorter than that of PPy-2 tubes. The well-dispersed PPy nanotubes suspension in ethanol forms free-standing PPy film when they were dried in the container at 60 °C. During the period of the evaporation of ethanol, the nanotubes spontaneously self-assembled into a piece of film with a uniform thickness. The SEM images of the different free-standing PPy membrane are shown in Fig. 3. Fig. 3a and c showed that the tangled PPy nanotubes aggregated to form such a membrane with an open porous network structure. The lengths are about 1–3 μm for PPy-1 tubes and 10 μm PPy-2 tubes. Fig. 3(b) and (d) displayed both cross-sectional images of PPy-1 and PPy-2 films, from which the thickness of both PPy films can be determined to be 200 μm. These images also showed that the bundles of PPy tubes twined together to form many layers, which further stacked together to produce the films. Clearly, the formation process of PPy films is a self-assembled progress. Compared with PPy-1 film, the tubes in PPy-2 film are more winding and bundling, which might hint that the conductivity and mechanical strength of PPy-2 film could be better than that of PPy-1 film.

The TE parameters of PPy-1 and PPy-2 films at 310 K were shown in Table 1. The conductivities (σ) of PPy-1 and PPy-2 membrane were about 3.43 and 9.81 S cm^{-1}, respectively. Fig. 4(a) shows the temperature dependence of electrical conductivities for PPy-1 and PPy-2 films. The conductivity of PPy-2 film is about 3 times higher than that of PPy-1 film. The PPy-2 film shows a good linear relationship between the $\ln(\sigma)$ and the $T^{-1/2}$, indicating that the charge transport of PPy-2 film follows the quasi-one-dimensional variable range hopping (1D-VRH) model (Eq. (1)):

$$\sigma(T) = \sigma_0 \exp[-(T_0/T)^{1/2}] \quad (1)$$

where σ_0 is a constant, T_0 is the characteristic Mott temperature that generally depends on the carrier hopping barriers [29].

Fig. 4(b) shows the temperature dependence of Seebeck coefficients (S) of two films. The Seebeck coefficient of PPy-2 film is slightly higher than that of PPy-1 film. The Seebeck coefficients of PPy-1 films have a maximum value (18.54 μVK^{-1}) at 350 K. The maximum Seebeck coefficient of PPy-2 films is18.84 μVK^{-1} at 370 K. The result of TGA (Fig. S3) showed that HCl-doped PPy film lost its dopants between 80 and 100 °C. And, the losing of dopants in the polymer can decrease the Seebeck coefficient of PPy films.

Both electrical conductivities and Seebeck coefficients of PPy-2 films are higher than those of PPy-1 films. These results imply that smaller diameters are helpful to approach larger conductivity and Seebeck coefficient of PPy nanotubes film. Such a result could also be attributed to the improved molecular ordering of polymer chains, which has also been proven by the results of XRD.

When the thermal conductivity of materials is similar, the power factor (PF) can be used to compare TE performance. It can be calculated by the following Eq. (2).

$$P = S^2\sigma \quad (2)$$

So the power factor of two PPy films was calculated in Table 1. The PF of PPy-2 is 0.31 $\mu Wm^{-1}K^{-2}$ at 310 K, which is about three times higher than that of PPy-1 films.

Because PPy films are too thin to measure their thermal conductivity, disk-like shape pellet made from the compression of PPy tubes were used for the measurement of their thermal conductivity. The temperature-dependent thermal conductivity of two

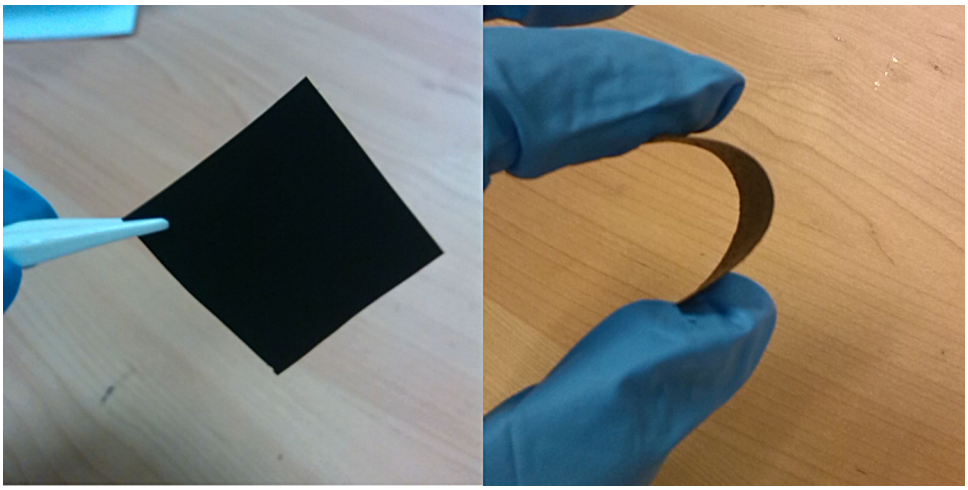

Fig. 1. Photographs of flexible free-standing PPy nanotube film.

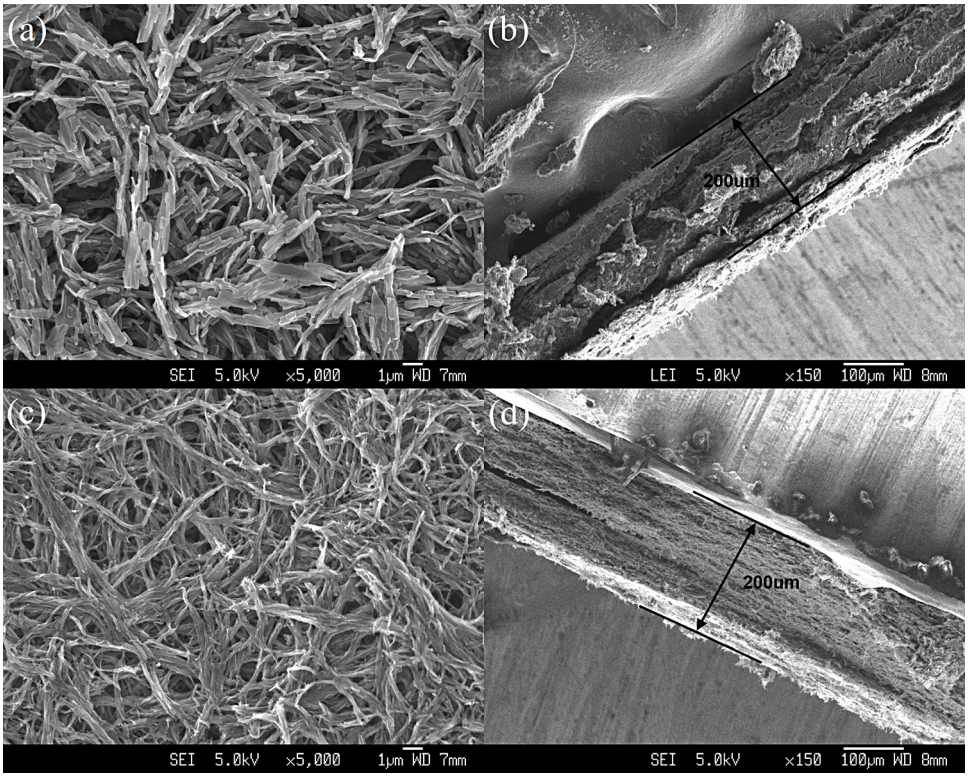

Fig. 2. (a–b) TEM images of PPy-1 tubes and (c–d) TEM images of PPy-2 tubes.

samples (Fig. 4c) showed that the thermal conductivity of two samples increased with the temperature rising and their value are close to each other.

The figure of merit, ZT (an important factor to evaluate TE materials) can be calculated by the following Eq. (3).

$$ZT = \left(\frac{S^2\sigma}{k}\right)T \tag{3}$$

where S is the Seebeck coefficient, T is absolute temperature, σ and k is electrical and thermal conductivity, respectively [30]. As shown in Fig. 4(d), the ZT values of PPy-2 film increases with the temperature rising. The ZT value of PPy-2 film is 5.71×10^{-4} at 310 K and ZT_{max} is 7.84×10^{-4} at 370 K. In the meanwhile, the ZT value of PPy-1 film is only 1.92×10^{-4} at 310 K and ZT_{max} is 2.53×10^{-4} at 350 K. Because of the higher conductivity and higher Seebeck coefficient

Table 1
The TE parameters of PPy-1 and PPy-2 films at 310 K.

	Conductivity (S cm^{-1})	Seebeck coefficient (μVK^{-1})	PF (μWm^{-1} K^{-2})	Thermoconductivity (Wm^{-1} K^{-1})	ZT (10^{-4})
PPy 1	3.43	16.51	0.09	0.15	1.92
PPy 2	9.81	17.68	0.31	0.17	5.71

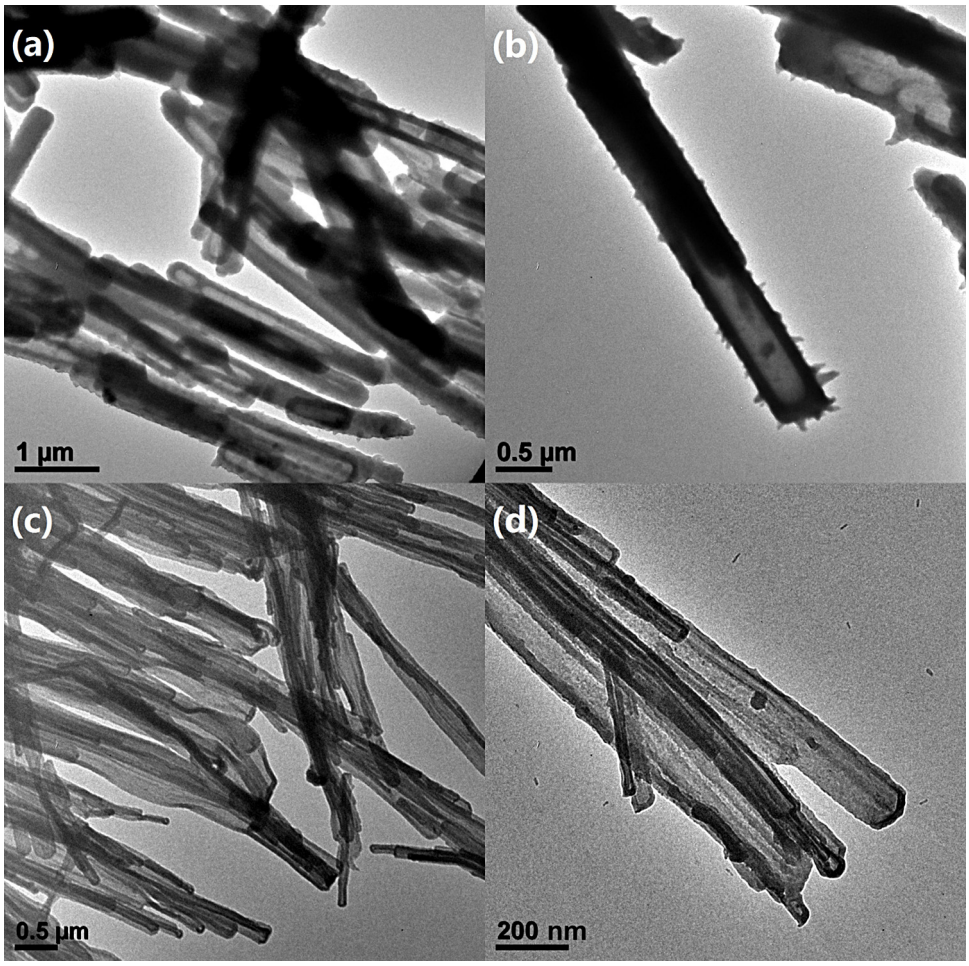

Fig. 3. (a) Surface and (b) cross-sectional SEM images of free-standing PPy-1 film, (c) surface and (d) cross-sectional SEM images of free-standing PPy-2 film.

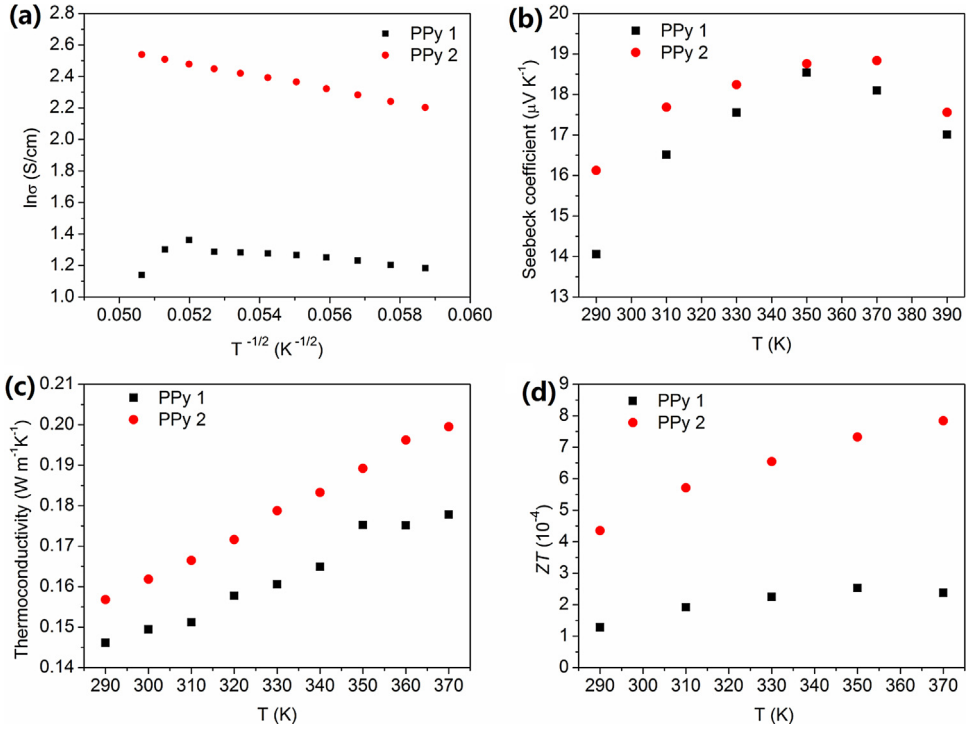

Fig. 4. The temperature (T) dependence of (a) electrical conductivity (σ); (b) Seebeck coefficient (S); (c) thermal conductivity; (d) figure-of-merit ZT of PPy-1 and PPy-2 films.

of PPy-2 film, the ZT_{max} value of PPy-2 films is about 3 times higher than that of PPy-1 film.

4. Conclusions

Two flexible free-standing PPy nanotube films were prepared and their morphologies and TE performances have been investigated. Since PPy-2 films have small diameter and longer length of nanotubes and the tubes in the same film are more winding and bundling, the conductivity and Seebeck coefficient of PPy-2 film are much higher than these of PPy-1 film. These results imply that smaller diameters and good molecular ordering of polymer chains are helpful to the larger conductivity and Seebeck coefficient. The ZT value of PPy-2 film is 5.71×10^{-4} at 310 K and ZT_{max} is 7.84×10^{-4} at 370 K, which is about 3 times larger than that of PPy-1 film. Compared to TE devices based on the typical inorganic/organic TE materials, the invention of TE device employing free-standing PPy nanotube films could benefit the production of low-cost flexible TE heating/cooling devices. The further enhancement of thermoelectric performance of PPy film through doping is still under investigation.

Acknowledgements

Q.Z. acknowledges financial support from AcRF Tier 1 (RG 16/12) and Tier 2 (ARC 20/12 and ARC 2/13) from MOE, the CREATE program (Nanomaterials for Energy and Water Management) from NRF, and the New Initiative Fund from NTU, Singapore. W.X. thanks the support from National Natural Science Foundation of China (21021091 and 21333011).

Appendix A. Supplementary data

Supplementary data associated with this article can be found, in the online version, at http://dx.doi.org/10.1016/j.synthmet.2014.08.001.

References

[1] K. Biswas, J. He, I.D. Blum, C.-I. Wu, T.P. Hogan, D.N. Seidman, V.P. Dravid, M.G. Kanatzidis, High-performance bulk thermoelectrics with all-scale hierarchical architectures, Nature 489 (2012) 414–418.
[2] G.J. Snyder, E.S. Toberer, Complex thermoelectric materials, Nat. Mater. 7 (2008) 105–114.
[3] K. Biswas, J. He, Q. Zhang, V.P. Dravid, G. Wang, C. Uher, M. Kanatzidis, PbTe–SrTe coherent endotaxial nanostructures with high thermoelectric figure of merit, Nat. Chem. 3 (2011) 160–166.
[4] K. Biswas, J. He, G. Wang, S.-H. Lo, C. Uher, V.P. Dravid, M.G. Kanatzidis, High thermoelectric figure of merit in nanostructured p-type PbTe–MTe (M = Ca, Ba), Energy Environ. Sci. 4 (2011) 4675–4684.
[5] Q. Zhang, C.D. Malliakas, M.G. Kanatzidis, $\{[Ga(en)_3]_2(Ge_2Te_{15})\}_n$: a polymeric semiconducting polytelluride with boat-shaped Te_8^{4-} rings and cross-shaped Te_5^{6-} units, Inorg. Chem. 48 (2009) 10910–10912.
[6] L.-D. Zhao, S.-H. Lo, Y. Zhang, H. Sun, G. Tan, C. Uher, C. Wolverton, V.P. Dravid, M.G. Kanatzidis, Ultralow thermal conductivity and high thermoelectric figure of merit in SnSe crystals, Nature 508 (2014) 373–377.
[7] R. Venkatasubramanian, E. Siivola, T. Colpitts, B. O'Quinn, Thin-film thermoelectric devices with high room-temperature figures of merit, Nature 413 (2001) 597–602.
[8] Y. Pei, X. Shi, A. LaLonde, H. Wang, L. Chen, G.J. Snyder, Convergence of electronic bands for high performance bulk thermoelectrics, Nature 473 (2011) 66–69.
[9] M. He, F. Qiu, Z. Lin, Towards high-performance polymer-based thermoelectric materials, Energy Environ. Sci. 6 (2013) 1352–1361.
[10] Y. Sun, Z. Wei, W. Xu, D. Zhu, A three-in-one improvement in thermoelectric properties of polyaniline brought by nanostructures, Synth. Met. 160 (2010) 2371–2376.
[11] Y. Sun, P. Sheng, C. Di, F. Jiao, W. Xu, D. Qiu, D. Zhu, Organc thermoelectric materials and devices based on p- and n-type poly(metal 1,1,2,2-ethenetetrathiolate)s, Adv. Mater. 24 (2012) 932–937.
[12] J. Wu, Y. Sun, W. Xu, Q. Zhang, Investigating thermoelectric properties of doped polyaniline nanowires, Synth. Met. 189 (2014) 177–182.
[13] Q. Zhang, Y. Sun, W. Xu, D. Zhu, Organic thermoelectric materials: emerging green energy materials converting heat to electricity directly and efficiently, Adv. Mater. (2014), http://dx.doi.org/10.1002/adma.201305371.
[14] N. Dubey, M. Leclerc, Conduting polymers: efficient thermoelectric materials, J. Polym. Sci. Part B: Polym. Phys. 49 (2011) 467–475.
[15] M.S. Dresselhaus, G. Chen, M.Y. Tang, R.G. Yang, H. Lee, D.Z. Wang, Z.F. Ren, J.P. Fleurial, P. Gogna, New directions for low-dimensional thermoelectric materials, Adv. Mater. 19 (2007) 1043–1053.
[16] M.G. Kanatzidis, Nanostructured thermoelectrics: the new paradigm? Chem. Mater. 22 (2009) 648–659.
[17] O. Bubnova, X. Crispin, Towards polymer-based organic thermoelectric generators, Energy Environ. Sci. 5 (2012) 9345–9362.
[18] W. Zhao, S. Fan, N. Xiao, D. Liu, Y.Y. Tay, C. Yu, D. Sim, H.H. Hng, Q. Zhang, F. Boey, J. Ma, X. Zhao, H. Zhang, Q. Yan, Flexible carbon nanotube papers with improved thermoelectric properties, Energy Environ. Sci. 5 (2012) 5364–5369.
[19] S.L. Kim, K. Choi, A. Tazebay, C. Yu, Flexible power fabrics made of carbon nanotubes for harvesting thermoelectricity, ACS Nano 8 (2014) 2377–2386.
[20] J. Xiang, L.T. Drzal, Improving thermoelectric properties of graphene/polyaniline paper by folding, Chem. Phys. Lett. 593 (2014) 109–114.
[21] K. Zhang, Y. Zhang, S. Wang, Enhancing thermoelectric properties of organic composites through hierarchical nanostructures, Sci. Rep. 3 (2013) 3448.
[22] E. Hu, A. Kaynak, Y. Li, Development of a cooling fabric from conducting polymer coated fibres: proof of concept, Synth. Met. 150 (2005) 139–143.
[23] Y. Du, S.Z. Shen, K. Cai, P.S. Casey, Research progress on polymer–inorganic thermoelectric nanocomposite materials, Prog. Polym. Sci. 37 (2012) 820–841.
[24] J.-S. Wu, D.-W. Gu, D. Huang, L.-J. Shen, Chemical in situ polymerization of polypyrrole nanoparticles on the hydrophilic/hydrophobic surface of SiO_2 substrates, Synth. React. Inorg. Metal-Org. Nano-Metal Chem. 42 (2012) 1064–1070.
[25] T. Peng, W. Sun, C. Huang, W. Yu, B. Sebo, Z. Dai, S. Guo, X.-Z. Zhao, Self-assembled free-standing polypyrrole nanotube membrane as an efficient FTO- and Pt-free counter electrode for dye-sensitized solar cells, ACS Appl. Mater. Interfaces 6 (2013) 14–17.
[26] X. Yang, Z. Zhu, T. Dai, Y. Lu, Facile fabrication of functional polypyrrole nanotubes via a reactive self-degraded template, Macromol. Rapid Commun. 26 (2005) 1736–1740.
[27] C. He, C. Yang, Y. Li, Chemical synthesis of coral-like nanowires and nanowire networks of conducting polypyrrole, Synth. Met. 139 (2003) 539–545.
[28] K. Cheah, M. Forsyth, V.T. Truong, Ordering and stability in conducting polypyrrole, Synth. Met. 94 (1998) 215–219.
[29] Z.H. Wang, E.M. Scherr, A.G. MacDiarmid, A.J. Epstein, Transport and EPR studies of polyaniline: a quasi-one-dimensional conductor with three-dimensional "metallic" states, Phys. Rev. B 45 (1992) 4190–4202.
[30] D.M. Rowe, Thermoelectrics Handbook Macro to Nano, CRC, Press, Taylor & Francis Group, Boca Raton, USA, 2005.